Article
JOURNAL OF UNIVERSITY OF BABYLON
For Pure and Applied Sciences (JUBPAS)
Vol. 34 ; No. 2| 2026

# Synthesized of Iron Oxide / Cobalt Oxide Nanocomposites Using Co-precipitation method, for Enhanced Removal of Malachite Green Dye via Adsorption

Alaa Salman Hussein [1*], Zainab Ghaleb Abdul Kareem [2], Abbas Jasim Atiyah [3] and Hussein Idrees Ismael [4]

1College of Education for Pure Sciences, University of Babylon, den155.alaa.salman@uobabylon.edu.iq, Hillah, Babylon, Iraq.
2College of Education for Pure Sciences, University of Babylon, den212.zanab.galab@uobabylon.edu.iq, Hillah, Babylon, Iraq.
3College of Sciences, University of Babylon, sci.abbas.jassim@uobabylon.edu.iq, Hillah, Babylon, Iraq.
4College of Sciences, University of Babylon, sci.hussein.edrees@uobabylon.edu.iq, Hillah, Babylon, Iraq.
***Corresponding author email:** den155.alaa.salman@uobabylon.edu.iq; mobile: 07708788554

# تحسين إزالة صبغة المالاكايت الخضراء عن طريق الامتزاز على مركبات نانوية مصنعة من أوكسيد الحديد مع أوكسيد الكوبلت

آلاء سلمان حسين[1*]، زينب غالب عبد الكريم[2]، عباس جاسم عطية[3]، حسين إدريس إسماعيل[4]

1 كلية التربية للعلوم الصرفة، جامعة بابل، den155.alaa.salman@uobabylon.edu.iq ، الحلة، بابل، العراق

2 كلية التربية للعلوم الصرفة، جامعة بابل، den212.zanab.galab@uobabylon.edu.iq ، الحلة، بابل، العراق

3 كلية العلوم، جامعة بابل، sci.abbas.jassim@uobabylon.edu.iq، الحلة، بابل، العراق

4 كلية العلوم، جامعة بابل، sci.hussein.edrees@uobabylon.edu.iq ، الحلة، بابل، العراق

**Accepted:** 25/6/2026 **Published:** 30/6/2026

## ABSTRACT

The current study involves the synthesis of iron oxide–cobalt oxide nanocomposites (FeO–CoO) in three different ratios (1:1, 2:1, and 1:2). These materials were synthesized using the co-precipitation method. The synthesized materials above were characterized by using different analytical and spectroscopic methods such as the X-ray diffraction technique (XRD), Field Emission Scanning Electron Microscopy (FESEM), Energy Dispersive X-ray Spectroscopy (EDX), BET surface area, and FTIR spectroscopy. Catalytic activity of the prepared materials was probed via screening removal of Malachite Green (MG) dye from simulated industrial wastewaters applying adsorption technique over these prepared materials. To screen adsorption efficiency many adsorption parameters were carried out. These including used weight of the materials, concentration of MG dye, acidity of the simulated polluted solution, and the effect of temperature of adsorption process. From the recorded findings, the best ratio of (FeO–CoO) nanocomposite materials was (2:1). This ratio showed the best removal activity in term of removing this dye over this material, this was around 85%, in case of using 0.20 g of catalyst, 20 ppm of MG dye, with acidic function of 6 and adsorption temperature at 25°C. In terms of adsorption isotherm, recorded results was fitted with adsorption model according to Freundlich adsorption isotherm. Activation energy was estimated according to Arrhenius plot, and it was around 23 KJ/mol. This value of energy falls in the range of physical adsorption.

**Keywords:** Adsorption processes, Wastewater treatment, Iron oxide, Cobalt oxide, Malachite Green dye.



مجلة جامعة بابل للعلوم الصرفة والتطبيقية مجلة جامعة بابل للعلوم الصرفة والتطبيقية

ISSN: 2312-8135 | Print ISSN: 1992-0652 | www.journalofbabylon.com | jub@itnet.uobabylon.edu.iq | info@journalofbabylon.com

ISSN: 2312-8135 | Print ISSN: 1992-0652
info@journalofbabylon.com | jub@itnet.uobabylon.edu.iq | www.journalofbabylon.com



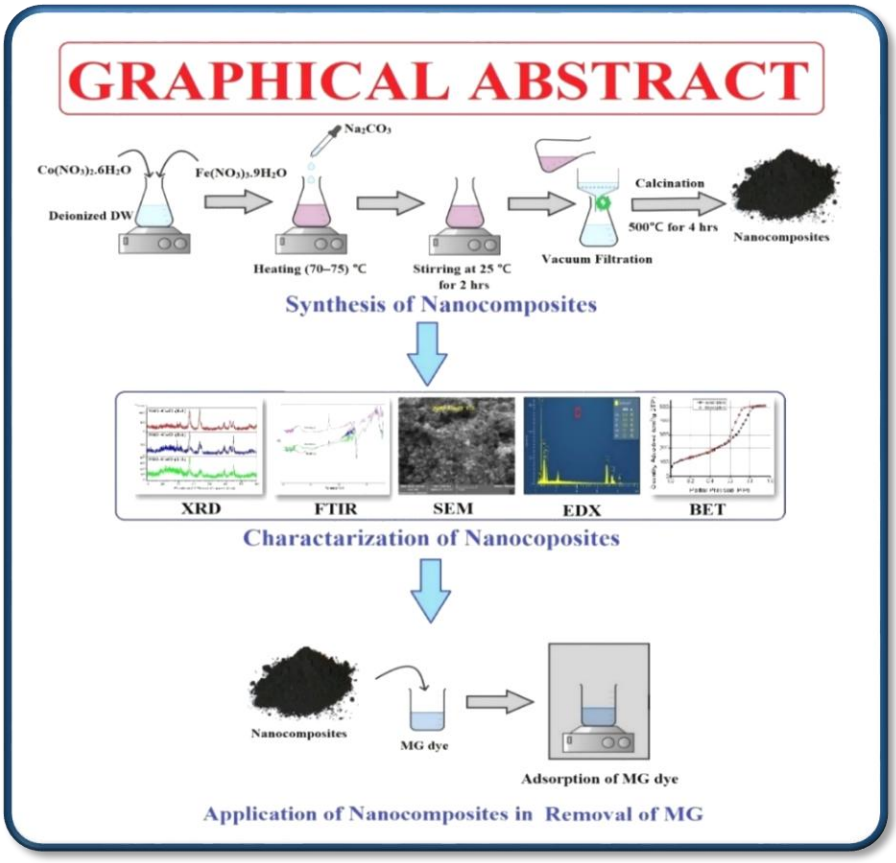


## INTRODUCTION

Supporting the increasing demand for potable water is a critical priority and remains a significant environmental challenge in the 21st century. The demand for water is rising owing to environmental change, overcrowding, industrialization, and ecological degradation [1, 2]. The significance of adsorption methods in the elimination of developing pollutants. Over 95% of emerging pollutants may be eliminated using adsorption. The adsorption efficiency may be enhanced by using nano adsorbents, metal oxide adsorbents, magnetic adsorbents, and hybrid adsorption processes for the removal of developing pollutant [3]. Nano adsorbents, nanometals, nanomembranes, and photocatalysts represent potential materials for tailored water technologies. The majority use contemporary treatment technologies and may be readily integrated. Contaminants in wastewater discharge, such as pesticides, dyes, plasticizers, disinfectants, polychlorinated biphenyls (PCBs), polycyclic aromatic hydrocarbons (PAHs), emerging contaminants, and endocrine disruptors, adversely affect health [4, 5]. The elevated surface areas and reactivity of novel nanomaterials render them promising for the elimination of hazardous contaminants. Eco-friendly methods for the extraction of ionic metal species from water have attracted interest. Nanotechnology and nanoscience, having progressed swiftly, provide several possibilities for water and wastewater treatment. Nanostructured materials are increasingly favored

ISSN: 2312-8135 | Print ISSN: 1992-0652
info@journalofbabylon.com | jub@itnet.uobabylon.edu.iq | www.journalofbabylon.com



for the degradation and remediation of harmful organic and inorganic contaminants owing to their distinctive attributes, such as elevated catalytic activity, stability, specific surface area, chemical reactivity, and electron transfer capability [6]. Dyes are chemical substances that adhere to surfaces or textiles to produce color. The bulk of dyes are complex chemical compounds that must exhibit resistance to many factors, including the effects of detergents. Synthetic dyes are extensively used throughout several sectors of modern technology including textiles, paper, leather tanning [7], food processing, plastics, cosmetics, rubber, printing [8, 9], and dye production industries. Synthetic dyes are used in groundwater tracking [10]. Due to its harmful consequences, aquatic dye pollution must be remedied immediately. Dyes' complex aromatic properties make them resistant to biological methods. Thus, chemical oxidation, advanced oxidation, coagulation/flocculation, membrane separation, and adsorption have been developed. Adsorption is a potential method due to its simplicity, absence of chemical agents, and lack of byproducts. Dye adsorption has been done using MOFs, carbon compounds, metallic substances, organic polymers, and their composites. Adsorbents with large surface areas and functional groups attract dye molecules and increase adsorption efficiency [11]. The oxides of nanomaterials containing iron (Ferrite) exhibit unique chemical and physical properties, such as superior magnetism, an extensive specific surface area, a high density of active sites on their surface, remarkable chemical stability, straightforward preparation, and adaptability to desired shapes, along with the potential for surface modification or functional group incorporation [12]. Consequently, it is included in the catalog of materials used as adsorbents, since it can be readily and swiftly extracted from the solution post-adsorption with the application of an external magnetic field. Upon separation, the contaminants may be extracted and reused several times, hence contributing to a reduction in water treatment expenses [13, 14]. Cobalt oxide is an established antiferromagnetic p-type multifunctional semiconductor characterized by a spinel crystal structure; the direct optical band gaps of $Co_3O_4$ nanoparticles are around 1.48 and 2.19 eV, making it an appropriate photocatalyst for the breakdown of organic contaminants under visible light. Cobalt, in its oxide forms, exhibits many spin states—high, low, and intermediate spin—rendering $Co_3O_4$ intriguing from a basic physics perspective, in addition to its potential in spintronic applications. These nanoparticles possess various important applications in fields such as field-effect transistors, energy storage, catalysis, anode materials for rechargeable lithium-ion batteries, electrochromic sensors, solar cells, and photocatalysis. Furthermore, these nanoparticles possess antibacterial, anticancer, antioxidant, antifungal, and enzyme inhibitory capabilities, owing to their exceptional biological applications [15].

Generally, MG dye is found as a solid material with a green powdered appearance, it is water soluble with high concentrations. This dye also called Leucomalachite Green dye, with a molecular formula of $C_{23}H_{26}N_2O$ [16, 17]. Malachite green (MG) dye is extensively used in several sectors such as cosmetics, tanning, textiles, printing, cotton, pigment manufacture, food processing, and rubber production. MG is a toxic cationic dye characterized by limited biodegradability and prolonged persistence in aquatic environments. It is regarded as a significant ocular irritant even in minimal quantities, in addition to being carcinogenic, genotoxic, mutagenic, and teratogenic

ISSN: 2312-8135 | Print ISSN: 1992-0652 | www.journalofbabylon.com | jub@itnet.uobabylon.edu.iq | info@journalofbabylon.com



[18]. The extensive application and unregulated discharge may result in several health issues, including respiratory enzyme toxicity, reduced erythrocyte count (anemia), and increased leukocyte levels, even at doses below 1 ppm [19].

The present work describes synthesis of (FeO – CoO) nanocomposites in three different composition ratios. The efficiency of prepared composites would be assessed by monitoring removal activity of MG dye from its simulated industrial wastewaters by adsorption over the prepared materials. This would also include evaluating various conditions and factors that might affect adsorption activity.

## MATERIALS AND METHODS

### Used Chemicals and Materials

The used chemicals in this work were Feric nitrate nonahydrate [$Fe(NO_3)_3.9H_2O$], this purchased from (THOMAS BAKER) with a purity of 98%, Cobalt (II) nitrate hexahydrate [$Co(NO_3)_2.6H_2O$] purchased from (Oxford Lab Chem) with a purity of 99%, Sodium carbonate [$Na_2CO_3$] purchased from (VWR INTERNATIONAL) with a purity 99.9%, hydrochloric acid [HCl] from (BDH) with 37% and Malachite Green dye powder (MG) with a molecular formula [$C_{23}H_{26}N_2O$], with a molar mass of 346.46 $mol.g^{-1}$, it was purchased from (BDH) company.

### Synthesis of Iron Oxide – Cobalt Oxide composite

Synthesis of this composite oxides was conducted using co-precipitation method, according to this method, a mixture of $Fe(NO_3)_3.9H_2O$ and $Co(NO_3)_2.6H_2O$ (in a different three ratios( 1:1, 1:2 and 2:1). This mixture was dissolved in 400 ml of deionized water at a constant stirring and under ambient atmospheric conditions. Controlling acidity of the solutions was kept around Ph=9 and it was performed using a digital pH meter. Adsorption temperature was kept around (70–75) ℃ with adding of $Na_2CO_3$ (1.0 M) as a precipitating agent drop wisely. Then the resulted mixture was kept undisturbed for 2 hours at room temperature with a constant stirring. A Buchner filtration flask equipped with a vacuum pump was used to remove the contaminants from the resulting combination. After that, the material was calcined at 500 ℃ for 4 hours at a heating rate of 100 ℃ per minute in an air environment [20]. Figure 2-3 shows schematic of procedure of synthesis of nanocomposite of Iron oxide – Cobalt oxide, characterization and application.

### Adsorption Study

In current study, adsorption processes were carried out applying batch methods, in each experiment a required amount of FeO–CoO composite was suspended in aqueous solution MG dye, 20 ppm in a volume of 100 ml. These experiments were conducted in a glass dual wall reactor kind, with a chiller (Julabo model EH/Germany). In all runs, adsorption mixture was kept homogeneously dispersed using a thermostatic magnetic stirrer (Heidolph MR Hei-Standard).

ISSN: 2312-8135 | Print ISSN: 1992-0652
info@journalofbabylon.com | jub@itnet.uobabylon.edu.iq | www.journalofbabylon.com



0.20 g of dye solution was suspended over composite oxides for every batch. After that, two milliliters of the solution were taken out every fifteen minutes, and the solid material was separated from the liquid supernatant by centrifugation. A UV-visible spectrophotometer double beam SHIMADZU (UV-Probe) was used to test the absorbance of clear liquid at a wavelength of 617nm. The activity of dye removal (R) from its solution was estimated using the following equation after each run lasted an hour:

$$Removal\ \% = \frac{(C_\circ - C_t)}{C_\circ} \times 100 \qquad (1)$$

From this relation, $C_0$ and $C_t$ represents initial dye concentration and its concentration at any time respectively [21]. Figure 1 shows UV- Visible Spectrum of MG dye obtain λmax of dye . A calibration curve for a series of MG dye concentrations ranging from 1 to 25 ppm was conducted using a maximum wavelength of this dye (617 nm) is shown in Figure 2.

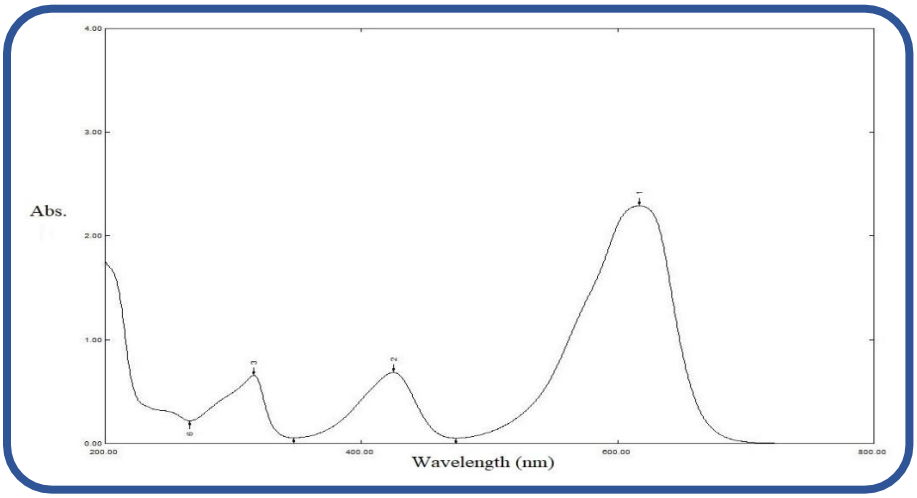


Figure 1: UV- Visible. Spectrum of MG dye

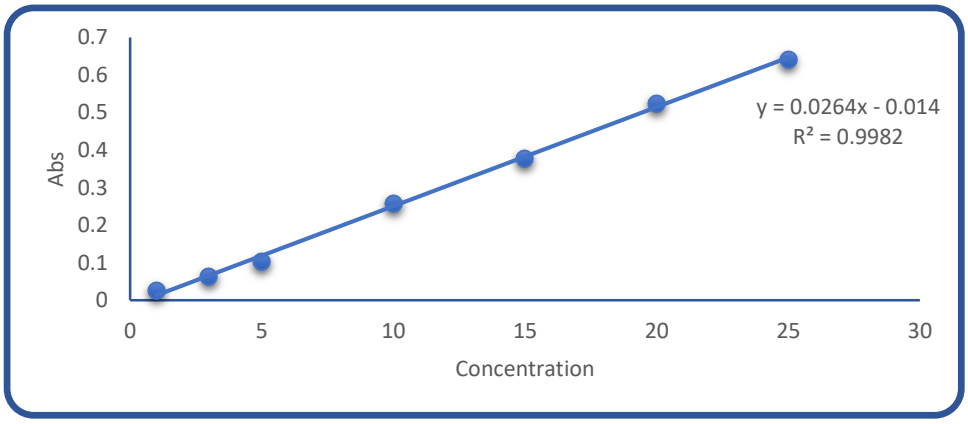


Figure 2: Calibration curve of MG dye (1 – 25) ppm.

مجلة جامعة بابل للعلوم الصرفة والتطبيقية مجلة جامعة بابل للعلوم الصرفة والتطبيقية

ISSN: 2312-8135 | Print ISSN: 1992-0652
info@journalofbabylon.com | jub@itnet.uobabylon.edu.iq | www.journalofbabylon.com

# RESULTS AND DISCUSSION

## Characterization of the Synthesized Nanomaterials

### X – rays Diffraction (XRD) of the Synthesized Nanomaterials

The XRD technique was used to characterize the crystalline phase of the Iron oxide/Cobalt oxide nanocomposites that were produced. Figure 3 shows the X-ray diffraction (XRD) patterns of Iron oxide/Cobalt oxide nanocomposites in three different ratios 1:1, 2:1 and 1:2. The detected peaks suggest the presence of the spinel phase of $FeCo_2O_4$. The peaks seen at 2θ values of 18.12, 30.27, 35.74, 43.47, 57.76, and 62.72◦ correspond to the (111), (220), (311), (400), (511), and (440) crystal planes of spinel $FeCo_2O_4$, as reported in earlier research [22-24]. From the obtained results, the crystallite sizes were around 12 nm for FeO–CoO (1:1), 10 nm for FeO–CoO (2:1) and 13 nm for FeO–CoO (1:2). So that, all the synthesized materials in the present study are full on nanometer scale.

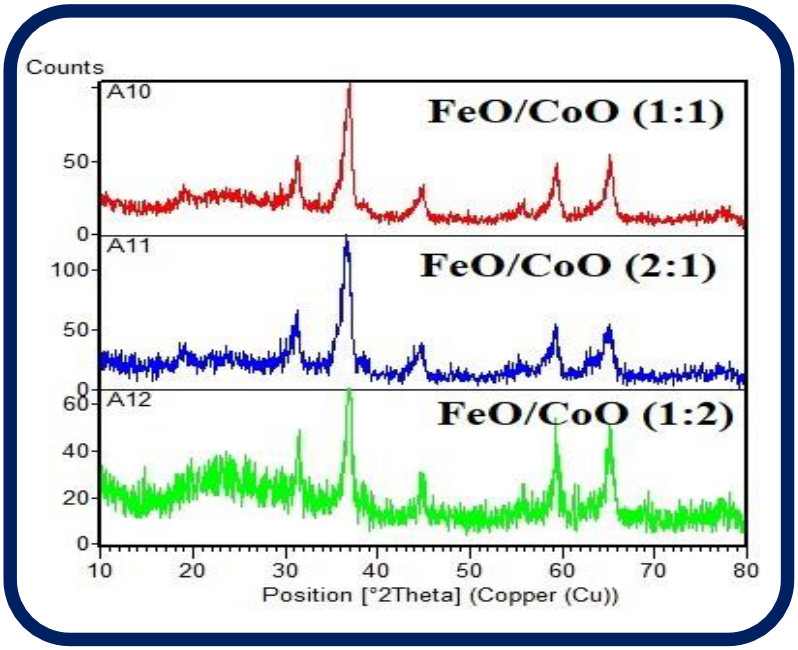


Figure 3: XRD Patterns of FeO – CoO Nanocomposites

### FTIR Spectra for Iron Oxide – Cobalt Oxide Nanocomposites:

Figure 4 shows the FTIR spectra of Iron oxide – Cobalt oxide nanocomposites in ratios of 1:1, 2:1, and 1:2. The FTIR analysis was performed at room temperature within a range of 400 to 4000 $cm^{-1}$ to study the chemical composition of Iron oxide – Cobalt oxide nanocomposites. The presence of metal oxide bands in spinel production is confirmed by the prominent peaks seen in FeO – CoO at around 400–650 $cm^{-1}$, such as at 418, 564, and 646 $cm^{-1}$. The three vibration bands of Fe–O and Co–O explain the inherent lattice vibrations and stretching of tetrahedral and octahedral coordination compounds in the spinel system. The bands are situated at about 1314 and

ISSN: 2312-8135 | Print ISSN: 1992-0652
info@journalofbabylon.com | jub@itnet.uobabylon.edu.iq | www.journalofbabylon.com



3413 $cm^{-1}$ as a result of water moisture adsorption. The absorption peaks in the nanocomposite demonstrate the presence of Iron oxide – Cobalt oxide nanocomposites [25, 26].

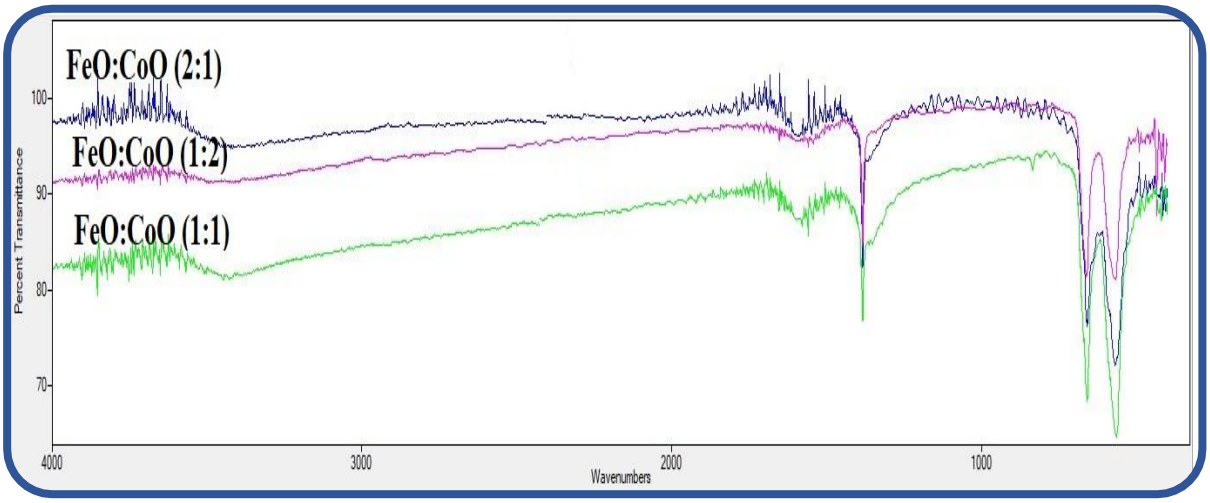


Figure 4: FTIR Spectra for FeO – CoO Nanocomposites

## FESEM for Iron Oxide / Cobalt Oxide Nanocomposites:

Investigation of surface morphology of the composite material screened using FESEM technique. The obtained images are presented in Figure 5. These images in general exhibit a spherical shape for the three different samples with relative aggregation for these for all samples. From these images, all samples have an average grain size which was around 27 nm for FeO – CoO (1:1), 26 nm for FeO – CoO (2:1) and 27 nm for FeO – CoO (1:2).

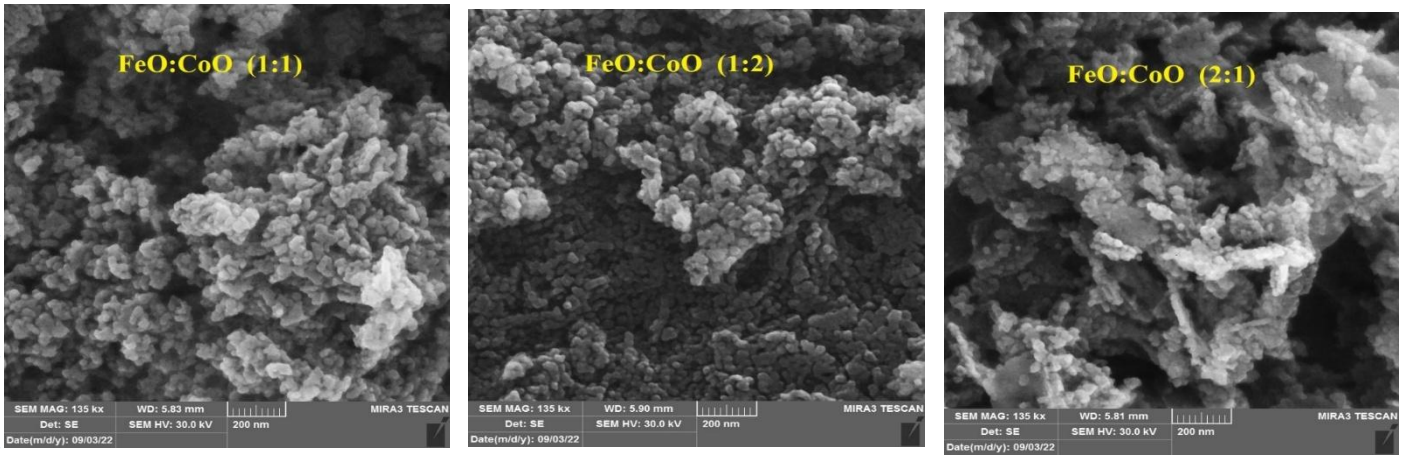


Figure 5: FESEM Images for the Nanocomposites of FeO – CoO

ISSN: 2312-8135 | Print ISSN: 1992-0652
info@journalofbabylon.com | jub@itnet.uobabylon.edu.iq | www.journalofbabylon.com



**DX for Iron Oxide – Cobalt Oxide Nanocomposites:**

The results of elemental analysis (EDX)for the prepared materials are presented in Figure 6, A, B and C for the samples, FeO – CoO (1:1) (A), (2:1) (B) and (1:2) (C) respectively.

These results show in Figure 6-A, a percent of 13.2 wt% of Iron, 39.3 wt% of Cobalt and 30.4 wt% of Oxygen. Figure 6- B, shows elemental composition of composites of Iron oxide and Cobalt oxide, FeO – CoO (2:1), it consists of 22.5 wt% of Iron, 51.3wt% of Cobalt and 18.8 wt% of Oxygen. Figure 6-C, shows elemental composition of a composite of FeO and CoO. For a composite's oxides, FeO – CoO (1:2), it consists of 12.0 wt% of Iron, 56.1 wt% of Cobalt and 21.1 wt% of Oxygen. Generally, from obtained results from EDX analysis, confirm exsistance of the proposed elements for all the synthesized materials in this study.

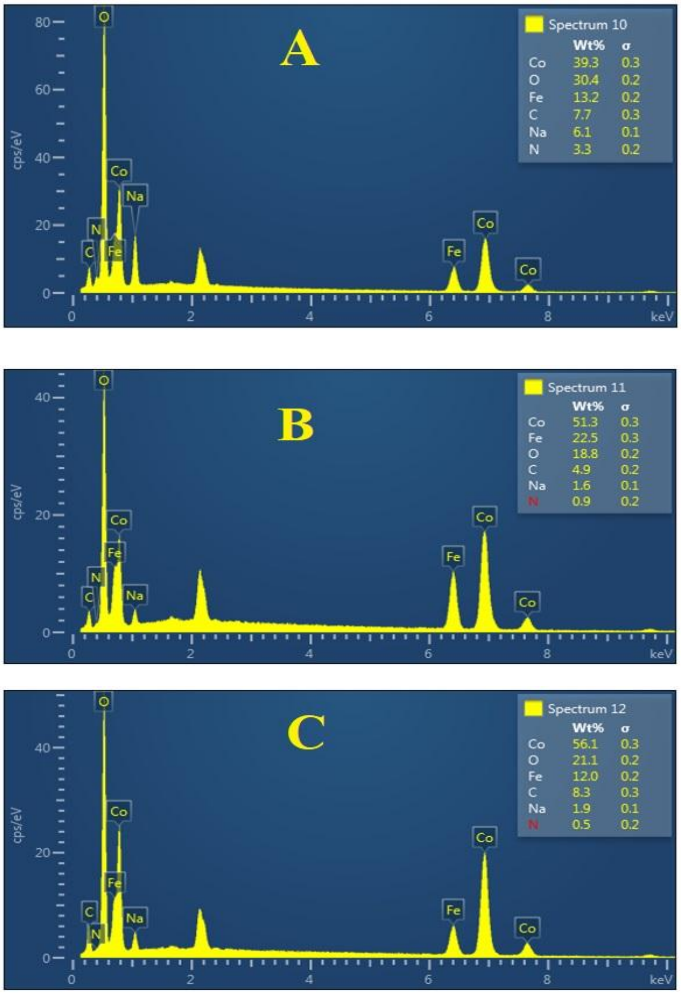


Figure 6: EDX Spectra for the Nanocomposites of FeO – CoO

A: FeO – CoO (1:1), B: FeO – CoO (2:1), C: FeO – CoO (1:2)

ISSN: 2312-8135 | Print ISSN: 1992-0652
info@journalofbabylon.com | jub@itnet.uobabylon.edu.iq | www.journalofbabylon.com



## BET specific surface area for the Synthesized Nanomaterials

BET surface area for the synthesized composite oxides was calculated applying the concept of physical adsorption of $N_2$ gas at 77 K using BET instrumentation and the recorded results are listed in Table 1. From the obtained results, it can be noted that, the synthesized composite oxide FeO–CoO in a ratio of (2:1) shows a bets BET surface areas in comparison with other ratios. There was a relative increase in surface area for this composite in comparison with other ratios. This can be related to high ratio of FeO in these composite oxides, this leads to an increase in the porosity of the resulted material which leads to an enhanced surface of this composite [27,28].

Table 1: BET Surface Area of Nanocomposites of Iron Oxide with Cobalt Oxide

| Catalysts | BET ($m^2$ / g) |
|---|---|
| **FeO – CoO (1:1)** | **41.2397** |
| **FeO – CoO (2:1)** | **46.1474** |
| **FeO – CoO (1:2)** | **45.2969** |

## Removal of MG Dye by Adsorption over Iron Oxide – Cobalt Oxide Nanocomposites:

The results of removal of MG dye by adsorption over FeO–CoO composite oxides are showed in Figure 7.

From these results, the best removal efficiency was over FeO / CoO in a ratio of (2:1) ratio and it was around 82%. This result can be related to its higher BET surface are in comparison with other composite oxides with other ratios. High surface for material is very important parameter in its adsorption activity as its related to having high numbers of adsorption sites that enable the surface to adsorb high numbers of adsorbate species [29]..

ISSN: 2312-8135 | Print ISSN: 1992-0652
info@journalofbabylon.com | jub@itnet.uobabylon.edu.iq | www.journalofbabylon.com



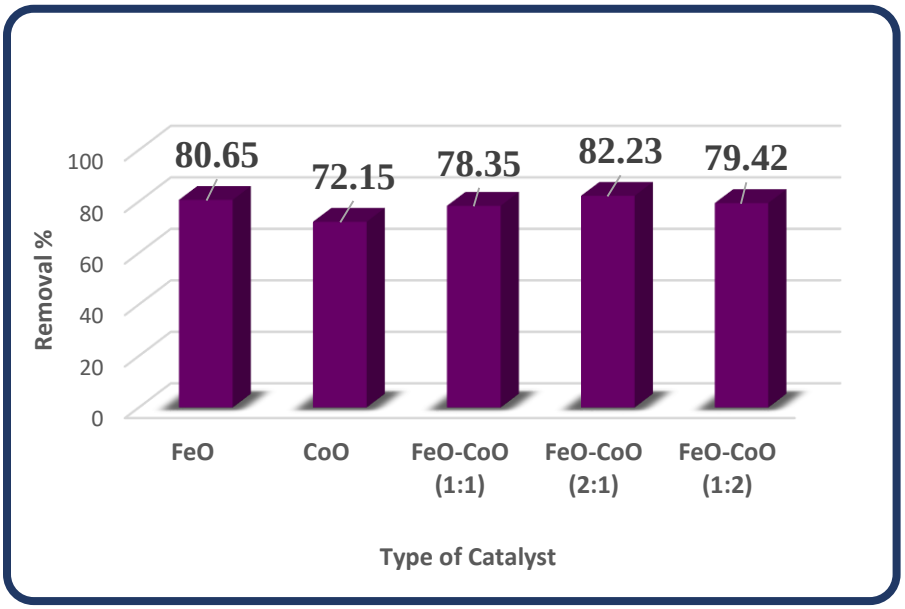


Figure 7: Removal Efficiency of MG Dye over Different Ratios of FeO – CoO Nanocomposites

## Effect Dosage of the Used FeO – CoO Adsorbent on the Efficiency of MG Dye Removal

The effect of amount of adsorbent on activity of MG dye removal by adsorption over a composite oxide (FeO–CoO) was investigated vi dispersing a series of masses of adsorbent with fixation all other adsorption conditions. The obtained results are showed in Figure 8. From these results, it can be noted that, there was a gradual increase in adsorption capacity with an increase in the amount of the used adsorbent from 0.05 g., and maximum removal efficiency was recorded at 0.2 g. after this value there was decrease in adsorption ability was noted. This observations are attributed to increase numbers of adsorption sites at the surface with increase amount of the adsorbent. This consequently leads to an increased number of adsorbed dye molecules [30]. On other hand, at high masses greater than (0.20 g.), reduction in adsorption capacity can be attributed to the reduction in adsorption sites due to aggregation of the adsorbent particles which leads to reducing the total number of accessible adsorption sites [31]. So, from the obtained results in this study it was found that, 0.2 g. was the maximum dose of FeO–CoO composite in this study which gives a maximum removal efficiency for the used which was around 85%.

ISSN: 2312-8135 | Print ISSN: 1992-0652
info@journalofbabylon.com | jub@itnet.uobabylon.edu.iq | www.journalofbabylon.com



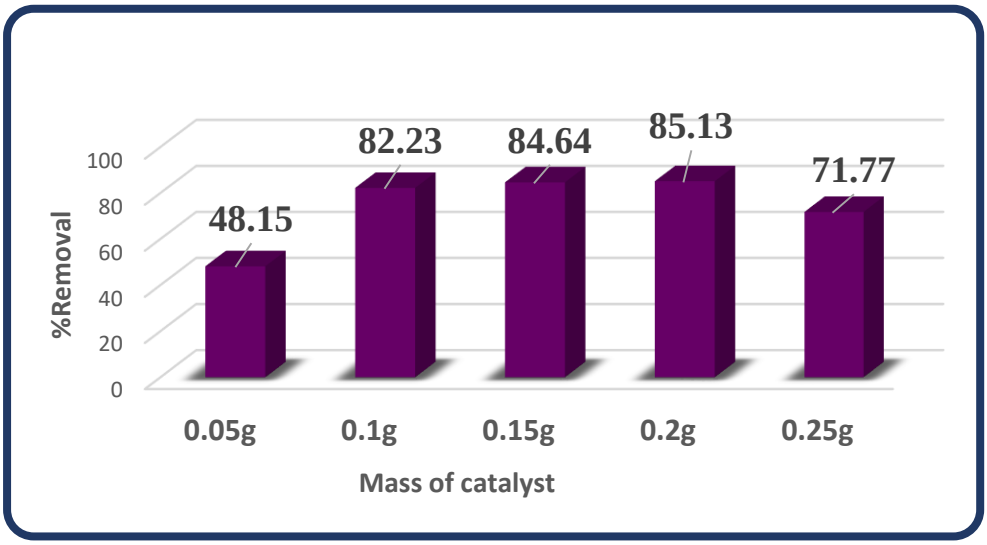


Figure 8: Effect of Using Different Dosages of FeO – CoO (2:1) on the Efficiency of MG dye Removal by Adsorption

**Effect of MG Dye Concentration on the Efficiency of its Removal over FeO – CoO (2:1) Nanocomposite:**

The effect of dye concentration on its removal efficiency by adsorption over FeO–CoO composite was investigated by applying a series of dye concentrations with the fixation of all other reaction conditions and the obtained results are shown in Figure 9.

The obtained results, showed an increase in activity of dye removal with an increase of dye concentration from 5 ppm up to 20 ppm, and maximum removal efficiency was recorded at dye concentration of 20 ppm. This observation is due to increase number of available dye molecules that are available to be adsorbed over the surface of the used adsorbent. After this concentration (20 ppm), there was a drop in the efficiency of dye adsorption with increase of dye concentration. This can be related to numerous additional increase in number of dye molecules competing for the same number of adsorption sites. In addition to that, increasing of dye concentration under these circumstances can lead to increase of viscosity of the solution. This can affect dye mobility which effect of the rate of diffusion of dye molecules from bulk solution towards adsorption sites at the surface of the used adsorbent [32].

ISSN: 2312-8135 | Print ISSN: 1992-0652
info@journalofbabylon.com | jub@itnet.uobabylon.edu.iq | www.journalofbabylon.com



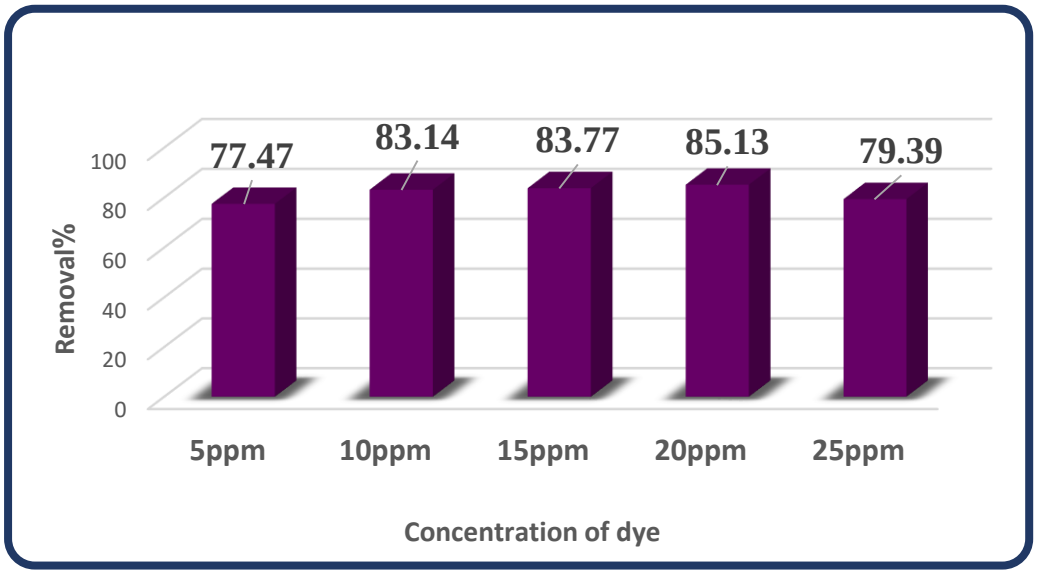


Figure 9: Effect of Using Different Concentrations of MG Dye on the Efficiency of its Removal over FeO – CoO (2:1)

## Effect of pH of MG Dye Solution on the Efficiency of its Removal:

The effect of acidity and basicity of dye solution on the activity of its adsorption over composite oxides (FeO–CoO) was investigated by conducting adsorption processes over a range of pH from pH= 2 to pH = 12 to predict a pH value that can yield maximum removal efficiency with fixation of all adsorption factors. The obtained results are shown in Figure 10. From these findings, it is clear that, MG dye removal efficiency was increased dramatically due to an increase in the pH value of dye solution from pH = 2 to pH = 6 to yield a best maximum removal efficiency at pH =2. After that, dye removal efficiency was reduced steadily from a neutral (7) to a high value of acidity of solution (pH=12), and the minimum adsorption capacity was recorded at a pH of 12.

These considerations, can be attributed to the effect of pH of solution on the net charge of the surface of the adsorbent. At acidic conditions, the surface of adsorbent would have a net positive charge, this can lead to increased electrostatic attraction between active sites of the surface and negatively charged groups of the dye, this would lead to an increased rate of diffusion of dye molecules from bulk towards these active sites and hence increase adsorption capacity. On other hand, under basic conditions electrostatic repulsion would occur as adsorbent surface has a net negative charge. This can lead to occur repulsion between dye molecules and adsorbent active sites which leads to reduce adsorption capacity of MG dye under these circumstances[33].

ISSN: 2312-8135 | Print ISSN: 1992-0652
info@journalofbabylon.com | jub@itnet.uobabylon.edu.iq | www.journalofbabylon.com



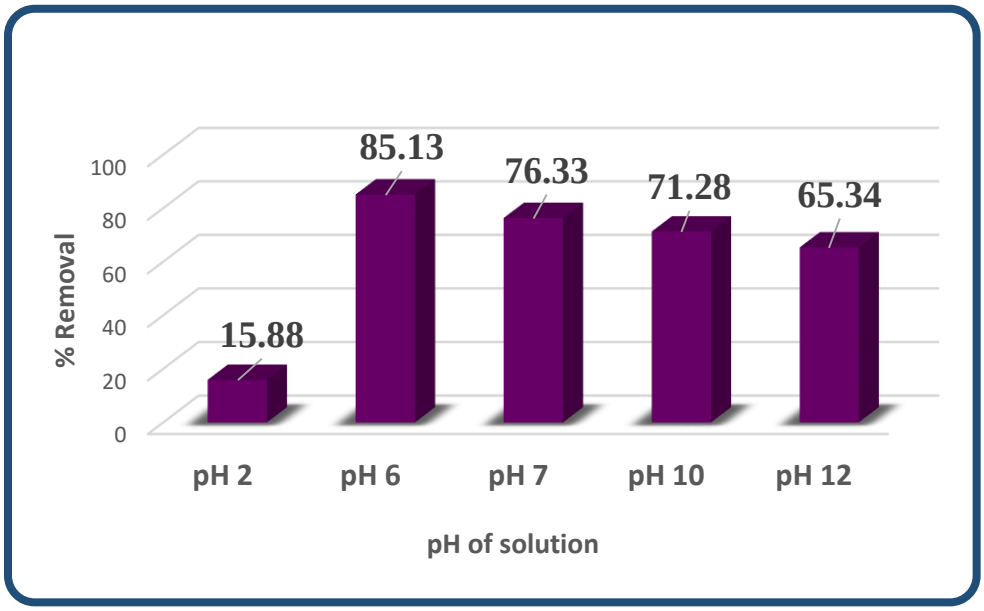


Figure 10: Effect of pH of Dye Solution on the Efficiency of its Removal over FeO – CoO (2:1)

## Effect of Temperature on the Efficiency of MG Dye Removal over FeO – CoO (2:1):

The effect of temperature on the adsorption capacity of MGG dye over FeO/CuO composite was screened by conducting adsorption processes under a series of temperatures ranging from 5 to 45 ℃, with an increase of temperature by 10 degrees between each interval with constant other adsorption conditions. The recorded results are shown in Figure 11, from these findings, it can be seen that, there was a gradual increase in adsorption capacity with elevation in temperature and the best removal efficiency was recorded at 25 ℃. This result can be related to increased kinetic energy of dye molecules and increase rate diffusion of dye molecules from bulk towards adsorption sites at the adsorbent surface which leads to increase adsorption efficiency under this condition. Additionally, increase in temperature can lead reduce the solution's viscosity which can lead to increased rate of diffusion of dye molecules from bulk towards adsorption sites at the adsorbent surface [34]. From other side, at temperatures greater than 25 ℃, there was a decrease in adsorption efficiency under the same adsorption conditions.

This observation can be related to a high increase in kinetics energy of dye molecules their ability to be adsorbed and this also can lead to desorb of dye molecules from adsorption sites into the bulk of solution. These circumstances can lead to reduced adsorption capacity for adsorption of dye molecules [35].

ISSN: 2312-8135 | Print ISSN: 1992-0652
info@journalofbabylon.com | jub@itnet.uobabylon.edu.iq | www.journalofbabylon.com



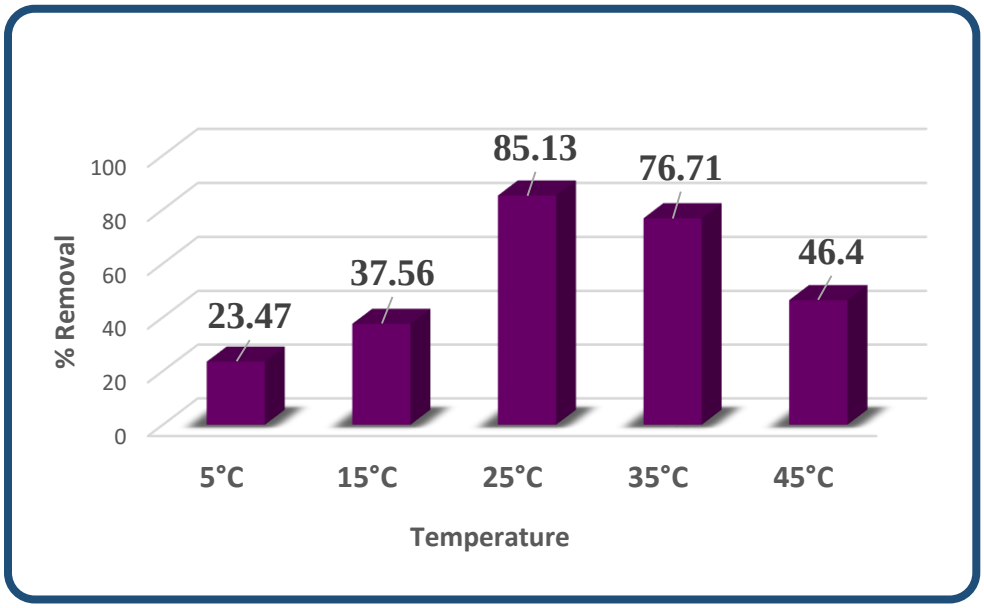


Figure 11: Temperature effect on the activity of Removing of MG dye over FeO – CoO (2:1)

Rate constant for the removal of MG dye by adsorption over composite oxides was estimated by plotting lnA◦/At against time of adsorption. This relation was applied by considering this process occurs according to pseudo first order kinetics. The recorded findings are shown in Figure 12 and are listed in Table 2. The value of rate constant ($k_1$ in $mim^{-1}$) for this process was calculated from the slope of the line that is obtained from linear relationship[36].

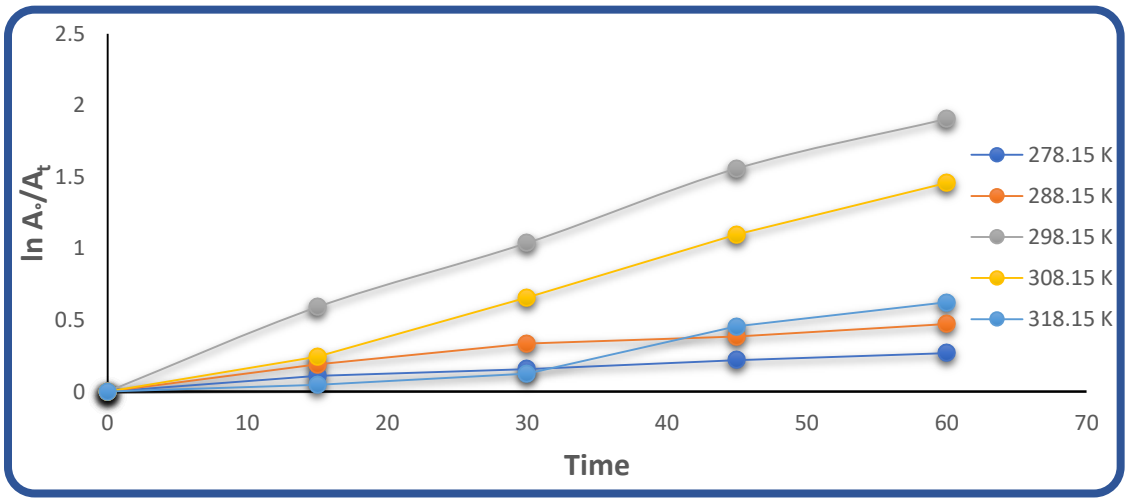


Figure 12: Evaluating rate constant for adsorption of MG dye over FeO – CoO (2:1) at different temperatures

ISSN: 2312-8135 | Print ISSN: 1992-0652
info@journalofbabylon.com | jub@itnet.uobabylon.edu.iq | www.journalofbabylon.com



Table 2: Rate constant values for adsorption of MG dye over FeO – CoO (2:1) at different temperatures

| Temperature (K) | Reaction rate constant K ($min^{-1}$) |
|---|---|
| **278.15** | **0.0043** |
| **288.15** | **0.0076** |
| **298.15** | **0.0319** |
| **308.15** | **0.0251** |
| **318.15** | **0.0110** |

**Calculation of activation energy for adsorption of MG dye over FeO – CoO (2:1)**

Activation energy (Ea) for adsorption of MG dye over FeO – CoO (2:1) was calculated by applying Arrhenius equation (2). The obtained results are summarized in Table 3 and are plotted in Figure 13.

$$\ln K = \ln A - \frac{Ea}{RT} \qquad (2)$$

Where K reaction rate constant ($min^{-1}$), A is Arrhenius factor, Ea is activation energy (kJ/mol), R is a universal gas constant = 8.314 (J/mol.K) and T is temperature (K) [37].

Table 3: Adsorption temperatures and rate constants for adsorption of MG dye over FeO – CoO (2:1)

| Temperature (K) | Reaction rate constant K ($min^{-1}$) | 1000/T | Ln K |
|---|---|---|---|
| **278.15** | 0.0043 | 3.595182456 | -5.449140256 |
| **288.15** | 0.0076 | 3.470414715 | -4.879607032 |
| **298.15** | 0.0319 | 3.354016435 | -3.445149269 |
| **308.15** | 0.0251 | 3.245172805 | -3.684887433 |
| **318.15** | 0.0110 | 3.14317146 | -4.509860006 |

ISSN: 2312-8135 | Print ISSN: 1992-0652
info@journalofbabylon.com | jub@itnet.uobabylon.edu.iq | www.journalofbabylon.com



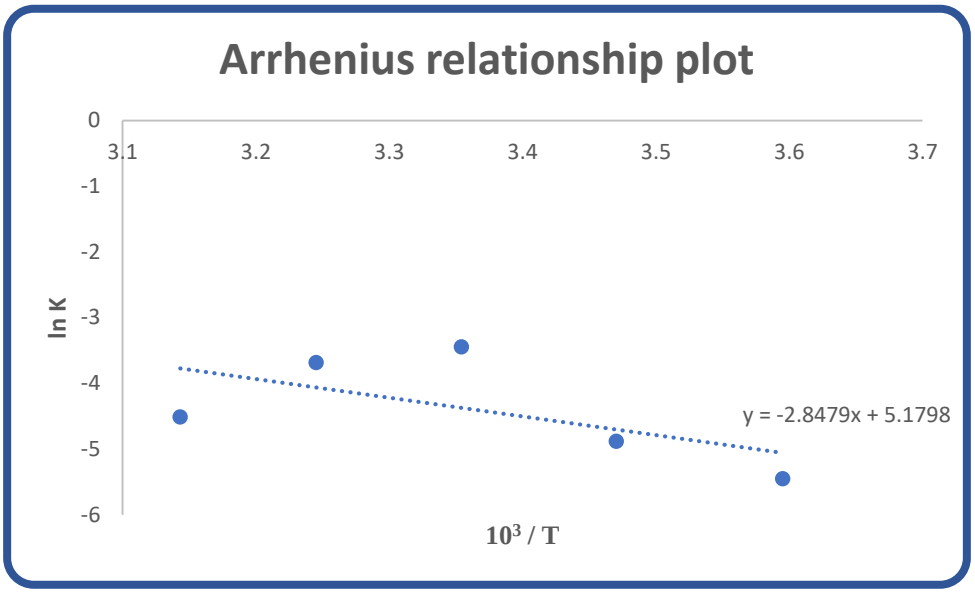


Figure 13: Arrhenius plot for adsorption of MG dye over FeO – CoO (2:1)

The estimated activation energy, derived from the data using the Arrhenius equation, was about 23.6774 kJ/mol. In this instance, the resulting activation energy is deemed minimal, falling within the range of physical energy activation, namely between 5 to 40 kJ/mol. Thus, it is reasonable to propose that physical adsorption happens in our investigation, with equilibrium being reached swiftly. Conversely, the activation energies for chemical adsorption are much larger, ranging from 40 to 800 kJ/mol. [38].

## Isothermal Study for Adsorption of MG Dye over FeO – CoO (2:1)

Adsorption isotherms quantitatively elucidate the interaction between contaminants in wastewater and their adsorption onto the surface of a chosen adsorbent, delineating the correlation between pollutant content in wastewater and its adsorption capacity. Employing this information is essential for enhancing the efficacy and design of adsorption-based treatment systems. The isotherms facilitate the selection and assessment of adsorbents by providing insights into their saturation points, efficacy, and adsorption capacity The optimization of adsorption systems is fundamentally dependent on the analysis of isotherm data through the application of various isotherm models for fitting. Several models exist for adsorption isotherms; however, for our study, we utilized the standard Langmuir and Freundlich models [39-41].

## Langmuir Isotherm

The fundamental premise of the Langmuir theory is that adsorption takes place at distinct homogeneous sites within an adsorbent, and once an adsorbate occupies a site, no additional adsorption can take place on that site. The model effectively predicts the performance of various adsorbents. A $K_L$ value, which is associated with the energy of sorption and indicates a high adsorption affinity, along with qm representing maximum adsorption capacity (i.e., monolayer

ISSN: 2312-8135 | Print ISSN: 1992-0652
info@journalofbabylon.com | jub@itnet.uobabylon.edu.iq | www.journalofbabylon.com



saturation), is known to decrease with increasing temperature. Langmuir adsorption isotherm can be presented in a linear form as follows:

$$\frac{C_e}{q_e} = \frac{1}{K_L\, q_m} + \frac{C_e}{q_m} \qquad (3)$$

From above relation, $C_e$ refers to concentration at equilibrium in bulk solution in (mg/L), $q_e$ refers to quantity of adsorbate per unit mass of adsorbent at equilibrium measured in (mg/g) is the amount of adsorbate per unit mass of adsorbent at equilibrium, $q_{m,}$ refers to theoretical amount of quantity of adsorbate for one layer at any time in (mg/g), and $K_L$, Refers to Langmuir constant that is related to heat of adsorption and it is measured in (L/mg). The values of each of $q_m$ and $K_L$ are calculated from the slope and intercept of the linear line that is obtained by plot of $C_e/q_e$ against $C_e$ . The obtained results are as plotted in Figure 14 and are listed in Table 4 [42, 43].

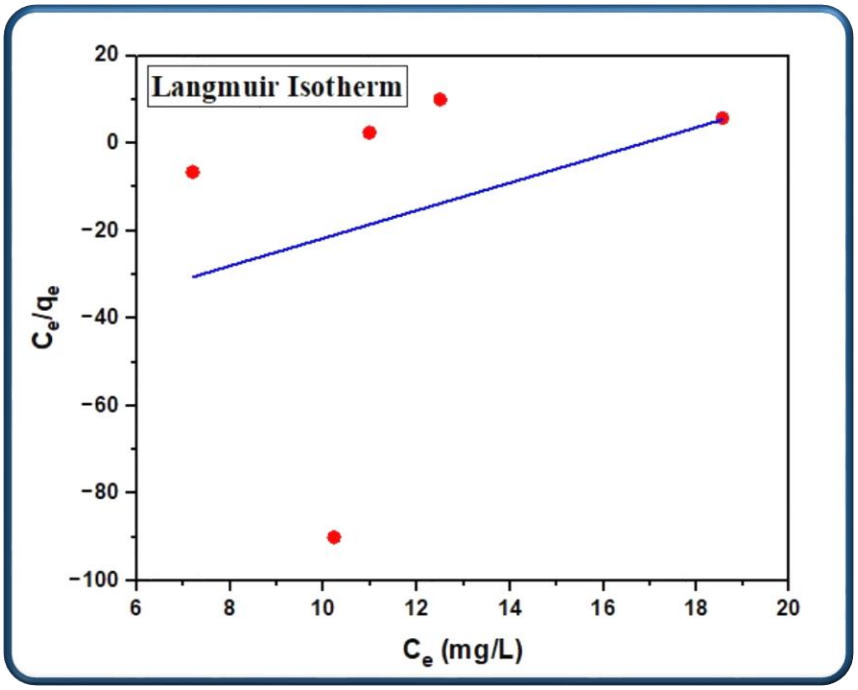


Figure 14: Langmuir Isotherm for Adsorption of MG Dye over FeO–CoO (2:1)

## Freundlich Isotherm

The Freundlich isotherm model characterizes adsorption as a phenomenon occurring on heterogeneous surfaces, involving a multilayer adsorption mechanism. The linear form of the Freundlich model is articulated as

$$q_e = K_F\, Ce^{1/n} \qquad (4)$$

$$Log\ q_e = \mathrm{Log}\, K_F + \frac{1}{n}\, Log\ C_e \qquad (5)$$

ISSN: 2312-8135 | Print ISSN: 1992-0652
info@journalofbabylon.com | jub@itnet.uobabylon.edu.iq | www.journalofbabylon.com



In this part, $K_F$ refers to Freundlich constant, 1/n refers to the adsorption intensity, $C_e$, refers to equilibrium dye concentration, and $q_e$ is the amount of adsorbate per unit mass of adsorbent at equilibrium. Freundlich coefficients n and $K_F$ can be obtained by plotting (Log $q_e$) against (Log $C_e$). When the value of n is between 1 and 10, it indicates favorable adsorption. The slope (1/n) serves as an indicator of adsorption intensity or surface heterogeneity when it falls between 0 and 1, indicating increased heterogeneity as its value approaches zero. Values below unity suggest a chemisorption process, with 1/n exceeding one indicating cooperative adsorption [44, 45]. These results are presented in Figure 15 and are listed Table 4.

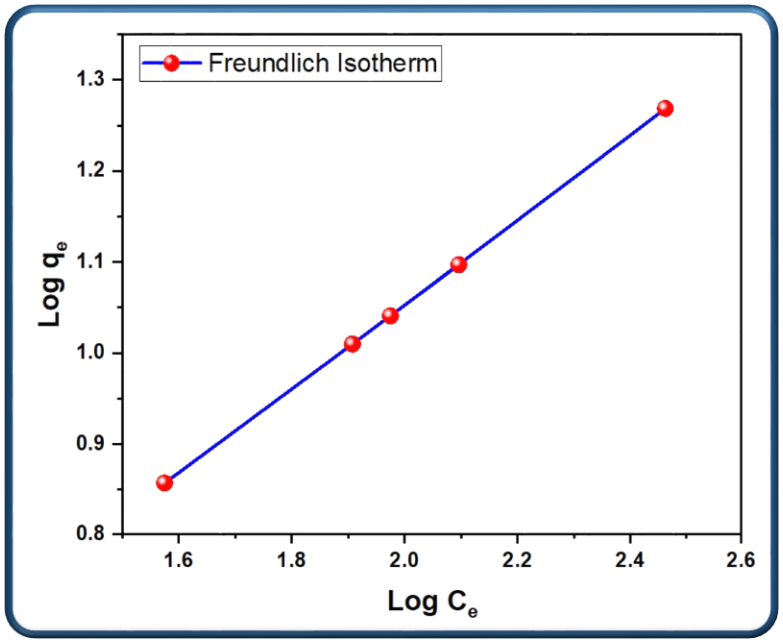


Figure 15: Freundlich adsorption isotherm for adsorption of MG dye over FeO–CoO (2:1)

Table 4: Langmuir and Freundlich constants for e adsorption of MG dye over FeO–CoO (2:1)

| Langmuir isotherm model | | | Freundlich isotherm model | | |
|---|---|---|---|---|---|
| $q_m$ (mg/g) | $K_L$ (L/g) | $R_L^2$ | $K_F$ | N | $R_F^2$ |
| **0.3159** | -0.0593 | 0.19991 | 0.5399 | 0.4645 | 0.999 |

The results indicate that, the correlation factor ($R^2$) derived from the Langmuir model is less than that obtained from the Freundlich isotherm. The findings indicate that the adsorption isotherm in this study aligns more closely with the Freundlich model.

ISSN: 2312-8135 | Print ISSN: 1992-0652 | www.journalofbabylon.com | jub@itnet.uobabylon.edu.iq | info@journalofbabylon.com



## CONCLUSIONS:

This study focused on the preparation of FeO–CoO composite oxides in three different ratios. The activity of these materials was examined by monitoring their absorption ability in removing MG dye from its aqueous solution by adsorption over these prepared materials. The obtained results, showed that the optimum adsorption capacity was recorded with a composite of FeO / CoO in a ratio of (2:1). In all cases, adsorption processes were performed using 0.2 g of the catalyst, at a concentration of 20 ppm of MG dye, at a pH = 6 and a temperature of 25℃. The best removal activity for dye adsorption was recorded under these conditions and it was around 85%.

adsorption isotherm investigation for the removal of MG dye by adsorption over FeO / CoO composite in a ratio of (2:1) was conducted using both the Langmuir and Freundlich models. From the found results, adsorption isotherm was more fitted with Freundlich model, confirming adherence to the Freundlich adsorption isotherm. The activation energy for the adsorption of MG dye over FeO / CoO in a ratio of (2:1) was estimated by applying the Arrhenius relation, and it was around 23 kJ/mol. This value is indicated that, it falls within the range of energetic requirements of physical adsorption.

## Acknowledgments:

Here in we would like to direct our full thanks to University of Babylon, College of Science for funding and supporting this work.

## Conflict of interests.

The authors declare that they have no known competing financial interests or personal relationships that could have appeared to influence the work reported in this paper.

## References

1. Karimi-Maleh, H., et al., *Novel 1-butyl-3-methylimidazolium bromide impregnated chitosan hydrogel beads nanostructure as an efficient nanobio-adsorbent for cationic dye removal: Kinetic study.* Environmental Research, 2021. **195**: p. 110809.
2. Abas, S.N.A., et al., *Adsorption process of heavy metals by low-cost adsorbent: a review.* World Applied Sciences Journal, 2013. **28**(11): p. 1518-1530.
3. Rathi, B.S. and P.S. Kumar, *Application of adsorption process for effective removal of emerging contaminants from water and wastewater.* Environmental Pollution, 2021. **280**: p. 116995.
4. Nasrollahzadeh, M., et al., *Green-synthesized nanocatalysts and nanomaterials for water treatment: Current challenges and future perspectives.* Journal of Hazardous Materials, 2021. **401**: p. 123401.
5. Zhang, W., D. Zhang, and Y. Liang, *Nanotechnology in remediation of water contaminated by poly- and perfluoroalkyl substances: A review.* Environmental Pollution, 2019. **247**: p. 266-276.
6. Xu, C., et al., *Benign-by-design nature-inspired nanosystems in biofuels production and catalytic applications.* Renewable and Sustainable Energy Reviews, 2019. **112**: p. 195-252.

7. Yagub, M.T., et al., *Dye and its removal from aqueous solution by adsorption: A review.* Advances in Colloid and Interface Science, 2014. **209**: p. 172-184.
8. Bensalah, N., M.A.Q. Alfaro, and C.A. Martínez-Huitle, *Electrochemical treatment of synthetic wastewaters containing Alphazurine A dye.* Chemical Engineering Journal, 2009. **149**(1): p. 348-352.
9. Dawood, S., T.K. Sen, and C. Phan, *Synthesis and characterisation of novel-activated carbon from waste biomass pine cone and its application in the removal of congo red dye from aqueous solution by adsorption.* Water, Air, & Soil Pollution, 2014. **225**: p. 1-16.
10. Field, M.S., et al., *An assessment of the potential adverse properties of fluorescent tracer dyes used for groundwater tracing.* Environmental Monitoring and Assessment, 1995. **38**: p. 75-96.
11. Shi, Y., et al., *A review on selective dye adsorption by different mechanisms.* Journal of Environmental Chemical Engineering, 2022. **10**(6): p. 108639.
12. Reddy, D.H.K. and Y.-S. Yun, *Spinel ferrite magnetic adsorbents: Alternative future materials for water purification?* Coordination Chemistry Reviews, 2016. **315**: p. 90-111.
13. Wadhawan, S., et al., *Role of nanomaterials as adsorbents in heavy metal ion removal from waste water: A review.* Journal of Water Process Engineering, 2020. **33**: p. 101038.
14. Alwan, E.K., et al., *Synthesis of cobalt iron oxide doped by chromium using sol-gel method and application to remove malachite green dye.* NeuroQuantology, 2021. **19**(8): p. 32-41.
15. Iravani, S. and R.S. Varma, *Sustainable synthesis of cobalt and cobalt oxide nanoparticles and their catalytic and biomedical applications.* Green Chemistry, 2020. **22**(9): p. 2643-2661.
16. Raval, A.R., H.P. Kohli, and O.K. Mahadwad, *Application of emulsion liquid membrane for removal of malachite green dye from aqueous solution: Extraction and stability studies.* Chemical Engineering Journal Advances, 2022. **12**: p. 100398.
17. Hussein, A.S. and N.Y. Fairooz, *Photocatalytic degradation of malachite green dye over naked niobium oxide as a photocatalyst.* Journal of University of Babylon, 2016. **24**(9).
18. Nath, J., S. Kumar, and V. Kumar, *Response surface methodology-based modeling and optimization of fenugreek gum-based hydrogel for efficient removal of malachite green dye.* Journal of Molecular Structure, 2023. **1293**: p. 136234.
19. Hussain, N., et al., *Engineered hybrid iron-cobalt metal oxide nanoparticles for effective adsorption of malachite green dye.* Journal of Chemical Technology & Biotechnology, 2024. **99**(12): p. 2553-2568.
20. Mohammad, E.J., A.J. Lafta, and S.H. Kahdim, *Photocatalytic removal of reactive yellow 145 dye from simulated textile wastewaters over supported (Co, Ni) O/AlO co-catalyst.* Polish Journal of Chemical Technology, 2016. **18**(3): p. 1-9.
21. Zhang, Y., et al., *Functional porous organic polymers with conjugated triaryl triazine as the core for superfast adsorption removal of organic dyes.* ACS Applied Materials & Interfaces, 2021. **13**(5): p. 6359-6366.
22. Manjula, N., V. Vinothkumar, and S.-M. Chen, *Synthesis and characterization of iron-cobalt oxide/polypyrrole nanocomposite: An electrochemical sensing platform of anti-prostate cancer drug flutamide in human urine and serum samples.* Colloids and Surfaces A: Physicochemical and Engineering Aspects, 2021. **628**: p. 127367.


مجلة جامعة بابل للعلوم الصرفة والتطبيقية مجلة جامعة بابل للعلوم الصرفة والتطبيقية

ISSN: 2312-8135 | Print ISSN: 1992-0652 | www.journalofbabylon.com | jub@itnet.uobabylon.edu.iq | info@journalofbabylon.com

23. Karimi-Maleh, H., et al., *A novel detection method for organophosphorus insecticide fenamiphos: Molecularly imprinted electrochemical sensor based on core-shell Co3O4@MOF-74 nanocomposite.* Journal of Colloid and Interface Science, 2021. **592**: p. 174-185.
24. Salame, P. and K. Kotalgi, *Ultrasonically assisted microwave synthesis of nanostructured FeCo2O4 as potential cathode materials for supercapacitors.* Journal of Materials Science: Materials in Electronics, 2020. **31**(22): p. 20072-20079.
25. He, X., et al., *Hierarchical FeCo2O4@polypyrrole Core/Shell Nanowires on Carbon Cloth for High-Performance Flexible All-Solid-State Asymmetric Supercapacitors.* ACS Sustainable Chemistry & Engineering, 2018. **6**(11): p. 14945-14954.
26. Parhizkar, J. and M.H. Habibi, *Investigation and Comparison of Cobalt ferrite composite nanoparticles with individual Iron oxide and Cobalt oxide nanoparticles in azo dyes removal.* Journal of Water and Environmental Nanotechnology, 2019. **4**(1): p. 17-30.
27. Xie, X., et al., *Arsenic removal by manganese-doped mesoporous iron oxides from groundwater: Performance and mechanism.* Science of The Total Environment, 2022. **806**: p. 150615.
28. Rehman, A., et al., *Nanostructured maghemite and magnetite and their nanocomposites with graphene oxide for photocatalytic degradation of methylene blue.* Materials Chemistry and Physics, 2020. **256**: p. 123752.
29. Barzinjy, A.A., et al., *Green and eco-friendly synthesis of Nickel oxide nanoparticles and its photocatalytic activity for methyl orange degradation.* Journal of Materials Science: Materials in Electronics, 2020. **31**(14): p. 11303-11316.
30. Pillai, P., et al., *Iron oxide nanoparticles modified with ionic liquid as an efficient adsorbent for fluoride removal from groundwater.* Environmental Technology & Innovation, 2020. **19**: p. 100842.
31. Hysna, F., et al., *Physically activated patchouli dregs carbon as a biosorbent for remotion of methylene blue.* Materials Today: Proceedings, 2023. **87**: p. 207-213.
32. Sultana, H. and M. Usman, *Surfactant-assisted flocculation for the efficient removal of aqueous dyestuff: A sustainable approach.* Journal of Molecular Liquids, 2023. **370**: p. 120988.
33. Hojjati-Najafabadi, A., et al., *Adsorptive removal of malachite green using novel GO@ZnO-NiFe2O4-αAl2O3 nanocomposites.* Chemical Engineering Journal, 2023. **471**: p. 144485.
34. Dehbi, A., et al., *Hematite iron oxide nanoparticles (α-Fe2O3): Synthesis and modelling adsorption of malachite green.* Journal of Environmental Chemical Engineering, 2020. **8**(1): p. 103394.
35. Alwan, S.H. and H.A. Alshamsi, *In situ synthesis NiO/F-MWCNTs nanocomposite for adsorption of malachite green dye from polluted water.* Carbon Letters, 2022. **32**(4): p. 1073-1084.
36. Elella, M.H.A., et al., *Green antimicrobial adsorbent containing grafted xanthan gum/SiO2 nanocomposites for malachite green dye.* International journal of biological macromolecules, 2021. **191**: p. 385-395.
37. Mohanty, N., S. Behera, and B.N. Patra, *Fabrication of Fe3O4/Polypyrrole/Phytic Acid Magnetic Nanocomposite for Preferential Adsorption of Cationic Dye: Adsorption Properties, Kinetics, and Mechanism.* Industrial & Engineering Chemistry Research, 2025.
38. Igwegbe, C.A., et al., *Adsorption of Congo red and malachite green using H3PO4 and NaCl-modified activated carbon from rubber (Hevea brasiliensis) seed shells.* Sustainable Water Resources Management, 2021. **7**(4): p. 63.


مجلة جامعة بابل للعلوم الصرفة والتطبيقية مجلة جامعة بابل للعلوم الصرفة والتطبيقية

ISSN: 2312-8135 | Print ISSN: 1992-0652 | www.journalofbabylon.com | jub@itnet.uobabylon.edu.iq | info@journalofbabylon.com

39. Selim, M.M., et al., *Addressing emerging contaminants in wastewater: Insights from adsorption isotherms and adsorbents: A comprehensive review.* Alexandria Engineering Journal, 2024. **100**: p. 61-71.
40. Hadi, A.A., et al., *Removal of Phenol Dye by CoFe2O4-CdFe2O4Nanocomposites.* IOP Conference Series: Earth and Environmental Science, 2021. **722**(1): p. 012023.
41. Obaid, S.A., *Langmuir, Freundlich and Tamkin Adsorption Isotherms and Kinetics For The Removal Aartichoke Tournefortii Straw From Agricultural Waste.* Journal of Physics: Conference Series, 2020. **1664**(1): p. 012011.
42. Kanagalakshmi, M., et al., *Adsorption Isotherms and Kinetic Models*, in *Carbon Nanomaterials and their Composites as Adsorbents*, J. Tharini and S. Thomas, Editors. 2024, Springer International Publishing: Cham. p. 135-154.
43. Salman Hussein, A. and A. Jasim Atiyah, *Removal of Malachite Green Dye by Adsorption over the Synthesized Composites of Iron Oxide and Nickel Oxide Nanoparticles.* Journal of Nanostructures, 2024. **14**(1): p. 295-310.
44. Zaheer, Z., A.-A. Aisha, and E.S. Aazam, *Adsorption of methyl red on biogenic Ag@ Fe nanocomposite adsorbent: Isotherms, kinetics and mechanisms.* Journal of Molecular Liquids, 2019. **283**: p. 287-298.
45. Rajahmundry, G.K., et al., *Statistical analysis of adsorption isotherm models and its appropriate selection.* Chemosphere, 2021. **276**: p. 130176.

ISSN: 2312-8135 | Print ISSN: 1992-0652
info@journalofbabylon.com | jub@itnet.uobabylon.edu.iq | www.journalofbabylon.com

## الخلاصة

تتناول هذه الدراسة تصنيع مركبات نانوية من أوكسيد الحديد وأوكسيد الكوبلت (FeO–CoO) بثلاث نسب مختلفة (1:1، 2:1، 1:2). تم تصنيع هذه المواد باستخدام طريقة الترسيب المشترك. وتم توصيف المواد المصنعة باستخدام طرق تحليلية وطيفية متنوعة، مثل تقنية حيود الأشعة السينية (XRD)، والمجهر الإلكتروني الماسح ذو الانبعاث الميداني (FESEM)، ومطيافية تشتت طاقة الأشعة السينية (EDX)، ومساحة السطح النوعية (BET)، ومطيافية الأشعة تحت الحمراء (FTIR). كما تم دراسة فعالية هذه المواد المصنعة من خلال إزالة صبغة المالاكايت الأخضر (MG) من محلولها المائي عن طريق الامتزاز على سطحها. وقد تم تطبيق ظروف ومعايير امتزاز مختلفة، مثل كتلة المحفز، وتركيز الصبغة المستخدمة، ودرجة حموضة المحلول، وتأثير درجة حرارة الامتزاز. أظهرت النتائج أن أفضل نسبة لمركبات FeO–CoO النانوية هي 2:1، حيث حققت أعلى كفاءة إزالة للصبغة المستخدمة، بلغت حوالي 85%. وقد تحقق ذلك باستخدام 0.20 غرام من المحفز، و20 جزءًا في المليون من صبغة المالاكايت الأخضر، ودرجة حموضة 6، ودرجة حرارة 25 درجة مئوية. كما أظهرت النتائج توافقًا أكبر مع معادلة فرندليش. حُسبت طاقة التنشيط بتطبيق معادلة أرينيوس للامتزاز، وبلغت حوالي 23 كيلوجول/مول، وهي ضمن نطاق الامتزاز الفيزيائي.

**الكلمات المفتاحية:** عمليات الإمتزاز، معالجة مياه الصرف الصحي، أوكسيد الحديد، أوكسيد الكوبلت، صبغة المالاكايت الأخضر.

ISSN: 2312-8135 | Print ISSN: 1992-0652
info@journalofbabylon.com | jub@itnet.uobabylon.edu.iq | www.journalofbabylon.com